Generation of 10-W average-power, 40-TW peak-power, 24-fs pulses from a Ti:sapphire amplifier system

H. Wang, S. Backus, Z. Chang, R. Wagner, K. Kim, X. Wang, D. Umstadter, T. Lei, M. Murnane, and H. Kapteyn

Center for Ultrafast Optical Science, University of Michigan, 2200 Bonisteel Boulevard, Ann Arbor, Michigan 48109-2099
(E-mail: sbackus@eecs.umich.edu)

Received May 3, 1999

We developed a compact, three-stage, multipass Ti:sapphire laser amplifier system that generates >40-TW pulses, with 24-fs pulse duration, at a repetition rate of 10 Hz, and with an average power of 10 W. Output intensities in excess of $1 \times 10^{19}\,\mathrm{W\,cm^{-2}}$ were produced. The technique of frequency-resolved optical gating was used to fully characterize the output pulses and to carefully compare theoretical models with experiment. High dynamic range frequency-resolved optical-gating measurements were performed, for the first time to our knowledge, to characterize the temporal wings of the output pulses. © 1999 Optical Society of America [S0740-3224(99)01010-3]

OCIS codes: 320.7090, 320.5520.

There has been rapid progress in the past four years in the development of terawatt-class ultrashort-pulse lasers with sub-~30-fs pulse durations.[1–7] This development has been motivated by scientific applications in high-field science, such as ultrafast coherent x-ray generation,[8,9] x-ray lasers,[10,11] and laser-based particle accelerators.[12,13] Many of these applications require high focused-pulse intensities, typically in excess of $10^{18}\,\mathrm{W/cm^2}$, in addition to a high peak-power requirement. However, high peak intensity can be achieved only if the beam quality from the laser amplifier system is close to diffraction limited.

In this paper we describe a compact tabletop Ti:sapphire laser system capable of generating >40-TW peak-power pulses, with 24-fs pulse duration, corresponding to an energy of 1 J per pulse at a repetition rate of 10 Hz. The average power of the system is 10 W. The beam focus of this multi-TW laser was carefully characterized, for the first time to our knowledge, with a high-dynamic-range CCD camera measurement. Optimal system designs allow us to maintain a low B integral and a compact size without compromising the system performance. We also compare the output from this laser system, which we carefully characterized using the technique of frequency-resolved optical gating[14] (FROG), with detailed models of the amplifier system. A high-dynamic-range FROG was performed, for the first time to our knowledge, to characterize the temporal wings of the output pulses. This paper represents the highest-power ultrashort-pulse laser system that has been fully characterized to date, to our knowledge.

The amplifier system is designed to be extremely compact, as shown in Fig. 1, covering an area of 6.5 $\mathrm{m^2}$. The source of the ultrashort seed pulses is a KLM Ti:sapphire oscillator pumped by a diode-pumped frequency-doubled solid-state laser (Spectra-Physics Millenia). The ~11-fs pulses from the oscillator are injected into a pulse stretcher, pulse selection, three stages of amplification, and a pulse compressor. The stretcher uses a folded-grating geometry consisting of one 1200-grooves/mm gold-coated grating and a spherical mirror (R = 812 mm), as shown in Fig. 2, that stretches the pulses to ~80-ps duration. The incidence angle to the grating is 37.8°, while the separation between the grating and its image is 20 cm. In a previous design[1] a parabolic mirror was used. However, we found that the parabolic mirror introduced errors in the group delay at the extreme edges of the spectrum, which became apparent when FROG was used to characterize the output. A ray-tracing analysis demonstrated that a spherical mirror was much closer to optimum for imaging the grating and that it is as close to aberration-free as the Offner triplet design.[15] The stretched pulses are then amplified in the first-stage amplifier, having reduced the repetition rate to 10 Hz with a Pockels cell. The first amplifier is a ring-cavity, eight-pass, Ti:sapphire amplifier[16] pumped with 19-mJ from a frequency-doubled YAG laser (Continuum YG681C). An aperture array of 2-mm-diameter holes within the three-mirror ring is used to reduce amplified spontaneous emission (ASE). The gain of the first amplifier is 10^6, while the output energy is 1.4 mJ.

After the first amplifier, the beam propagates through a spatial filter, through a second Pockels cell (used to isolate the first amplifier from backreflections), and then into the second amplifier stage. The spatial filter uses two 0.5-m focal-length lenses with a 200-μm diamond pinhole at the focus point. The second amplifier consists of four passes pumped by the remaining 330 mJ from the Continuum YAG laser. The pump beam is relay imaged onto the Ti:sapphire crystal. The output energy of the second amplifier is 100 mJ. The output beam then

0740-3224/99/101790-05$15.00

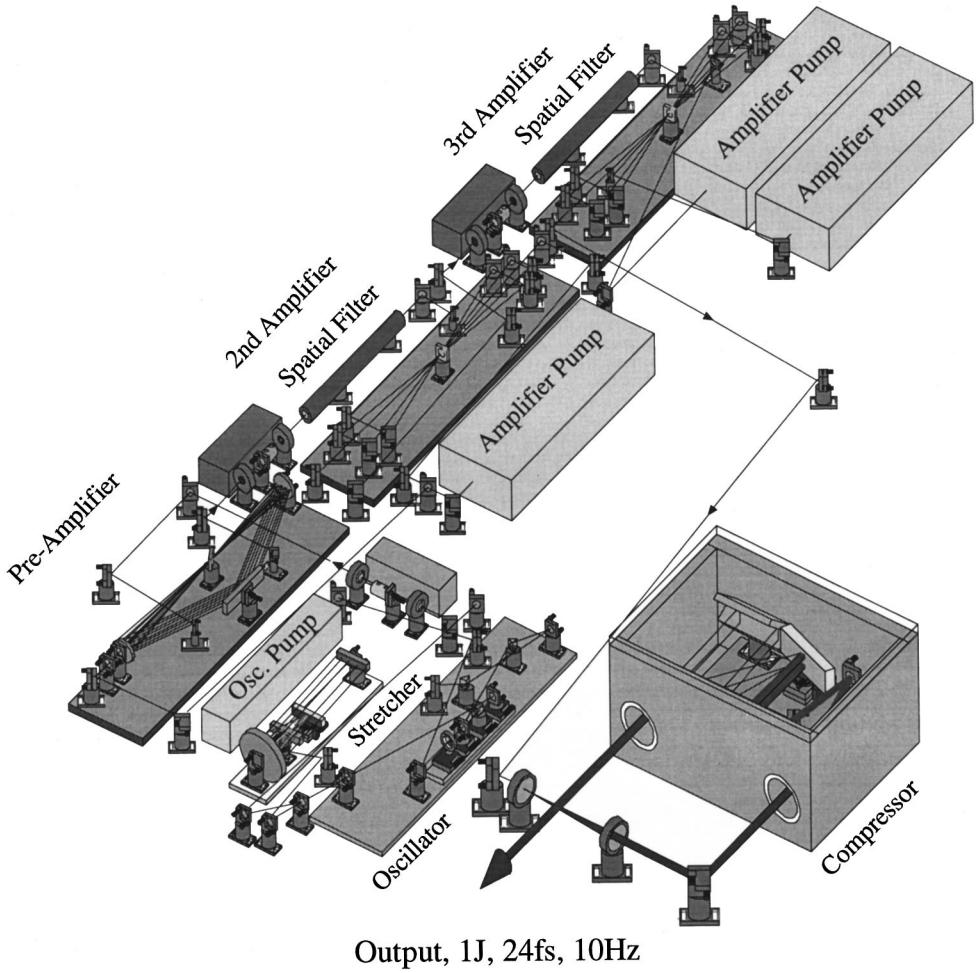

Fig. 1. Schematic diagram of the 10-Hz, 40-TW peak-power laser. The system occupies a space of 6.5 m^2 total.

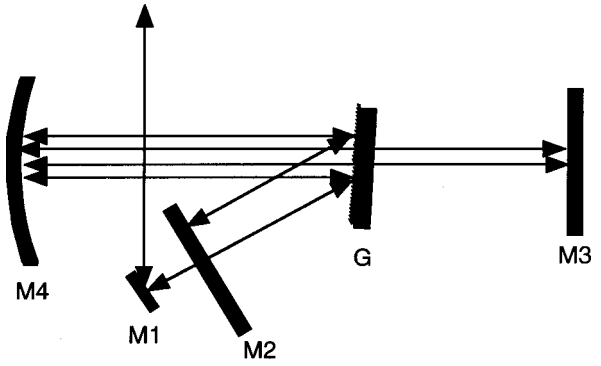

Fig. 2. Schematic diagram of the stretcher, where G is a grating, M1, M2, and M3 are flat mirrors, and M4 is a spherical mirror.

propagates through a vacuum spatial filter that also expands the beam to 12 mm in diameter. The pinhole of the spatial filter is selected to be twice the diffraction-limited focused spot size and is manufactured by drilling a hole through a negative fused-silica lens. A final Pockels cell is used to isolate the second and the third amplifier stages to prevent damage to the amplifier from back-reflected light from an experiment. The beam energy is reduced to 70 mJ as a result of losses from the spatial filter and the final Pockels cell.

The third amplifier stage uses a four-pass scheme. It is pumped on each side by 1.4 J from a frequency-doubled YAG laser (Spectra-Physics GCR350) operating at a repetition rate of 10 Hz. The pumped area on the crystal is 12 mm in diameter, resulting in a total pump fluence of 2.5 J/cm^2. The Ti:sapphire crystal used in this third and final amplifier stage is 20 mm in diameter and 10 mm long and is doped at a concentration of 0.15%. This concentration is less than the 0.25% doping used in the first two amplifier stages to reduce the possibility of gain depletion owing to ASE. The sides of the crystal were also coated with black paint to further reduce depletion caused by transverse lasing.

Under saturation conditions the near-field output beam profile from the third amplifier resembles that of the flattop pump beam profile. This is not desirable because only 76.6% of the energy falls within the $1/e^2$ radius of the focal spot for a flattop beam, compared with 86.5% for a Gaussian spatial profile beam. Moreover, diffraction rings develop quickly in the case of a flattop beam, which is very undesirable because of potential damage to the gratings and because of beam nonuniformity for application experiments. To generate a near-Gaussian beam profile under saturation conditions, one inserts a diverging lens after the mode-matched first pass through the

third amplifier. The beam then slowly diverges to 16 mm by the exit of the amplifier. The resulting near-field output beam profile is then very close to Gaussian, as discussed below. The output energy is 1.34 J, corresponding to a total gain of approximately 20 from the third amplifier stage, or an efficiency of 45%. This compares well with the maximum value of 66% that in theory can be extracted from such an amplifier. It also compares well with previously published work that reports similar values for efficiency (45%) for 10-TW pulse generation[5] and 33% efficiency for 25-TW pulse generation.[2]

Following amplification, the beam from the third stage is expanded to 4-cm diameter before compression with a pair of 1200-grooves/mm gold-coated gratings (Richardson Grating Labs #1570-1), blazed at 600 nm. The grating separation is 21 cm, and the angle is 40.3°. This compact compressor design is contained within a modest-size, table-top vacuum chamber (90 cm × 40 cm). The main limitation on the compression efficiency is the diffraction efficiency of the gratings themselves, which is 94%. The net compression efficiency (including mirrors in the compressor) is 75%, resulting in a compressed pulse energy of 1 J.

All of our system parameters, such as pump fluence, beam diameter, grating angles, and separation, were first calculated and optimized with a model that propagates the oscillator pulse through the optical system and includes the effects of gain narrowing, gain saturation, spectral shaping, dispersion of all materials, mirrors, and gratings, and gain dispersion. Exact expressions for the spectral phase were used, or, if unavailable, the group delay of an optic was measured experimentally and then used in our amplifier model. In the ideal case of complete dispersion compensation the relationship between the phase and the frequency is linear. When we minimize the dispersion, we first make the best linear fit (smallest mean-square error) to the phase as a function of frequency for a set of system parameters, for example, the incidence angles and the separations of the stretcher and the compressor. The system parameters are then adjusted to minimize the mean-square error so that the phase is most linear with the frequency. We find that this method gives better results than minimization of the high-order terms at the center frequency in a Taylor series expansion of the phase as a function of frequency.

The pulse duration was measured and optimized with the technique of second-harmonic FROG.[14,17] The measured amplitude and phase of the 24-fs output pulse is shown in Fig. 3, together with our model predictions. The pulse is near transform limited, with a small amount of uncompensated fourth-order dispersion remaining. In the future this uncompensated dispersion will be eliminated with either a prism pair or programmable phase compensation with deformable mirrors or liquid-crystal devices.[18,19] The peak output power from the amplifier is >40 TW. The center wavelength of the input spectrum is peaked at 780 nm and was specifically chosen to maximize the final output amplified bandwidth of 38 nm FWHM. The combination of gain narrowing and gain saturation shifts the final output spectra to the red with respect to the input. ASE was also measured with a fast photoswitch and neutral-density filters. The ASE intensity is at approximately the 10^{-5} level. The ASE energy is ~0.5% of the total energy.

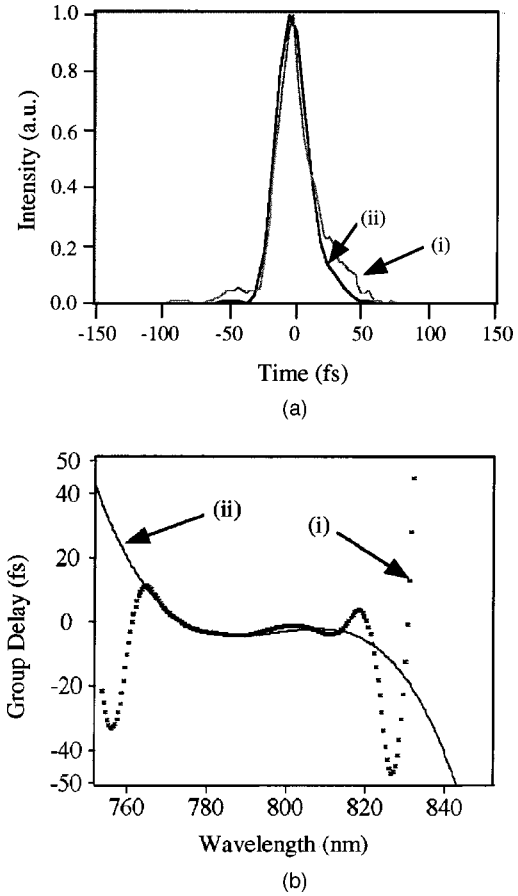

Fig. 3. (i) Measured and (ii) predicted (a) pulse shape and (b) group delay of the compressed output pulses with FROG.

Knowledge of the pulse contrast ratio (peak to wings) is essential for a high-peak-power ultrafast laser. We performed a high-dynamic-range second-harmonic FROG measurement to characterize the temporal wings. Although the CCD camera used in our FROG setup is 16 bit, the dynamic range of the CCD camera is still the main limitation that prevents us from measuring the temporal wings of the pulse down to 10^{-5} of the peak intensity. We thus made two measurements with different exposure times to increase the dynamic range of the raw data. One measurement was done with the normal exposure time, and the other measurement was done with a longer exposure time, which of course saturated the camera around the peak region. We then replace the saturated part of data of the latter measurement with the corresponding data taken in the former measurement by multiplying the ratio of the different exposure times. Our high-dynamic-range FROG measurement demonstrates that the full width at 10^{-5} of the peak intensity is ~400 fs, as shown in Fig. 4. The energy inside the wings is not significant.

To achieve the highest possible focused peak intensity, the beam quality must be good. A high-dynamic-range detector must be used to determine the true output beam quality and focusability because the energy outside the $1/e^2$ focal-spot radius is comparable to the energy inside

the focal spot, although the intensity may be many orders of magnitude lower. We used a 16-bit CCD camera to measure the far-field compressed output beam. The beam was first focused by a 600-mm off-axis parabola at full power and at a full beam diameter of ~4 cm. The focal spot was then imaged onto the CCD camera. Several uncoated wedged blanks and neutral-density filters were used in the imaging system to reduce the intensity. Figure 5(a) shows the near- and far-field compressed output beam profiles. The measured $1/e^2$ radius of the focal spot was 9.4 μm, corresponding to 1.2 times the theoretical diffraction limit. We can also determine, by integrating over the high-dynamic-range focal-spot image, that 44% of the beam energy lies within the $1/e^2$ radius of the focal spot, as shown in Fig. 5(b). This is the first time such a measurement has been reported at the 40-TW power level, to our knowledge. The peak intensity is therefore 1.4×10^{19} W/cm^2. Given the excellent beam quality, higher peak intensity is easily accessible if a shorter-focal-length parabola is used. The actual beam quality may be considerably better than measured, considering a number of possible aberrations in the imaging system such as flatness of the wedged blank and aberrations in the imaging system. We also varied the output energy from a few millijoules to full power. No change at the focal spot was observed. This shows that *B*-integral and thermal-lensing aberrations are negligible.

Several design aspects of this laser system contrast with previous ultrahigh peak-power Ti:sapphire laser systems. The relatively modest pulse stretching (~80 ps) in this system can be accommodated because of the limited total material path length (~36 cm) in the system. Given the output fluences at various stages in the amplifier system, the calculated *B* integral $[=2\pi/\lambda(\int n_2 I \mathrm{d}x)]$ is 1 rad. This value is sufficiently low to allow excellent focusability and recompression of the pulses, as we demonstrated. The relatively low stretch factor allows us to propagate a large spectral bandwidth (150 nm) through the stretcher/compressor, which avoids pulse distortion that is due to spectral clipping. It also helps to reduce effects that are due to imperfection of the gratings. The physical sizes of the stretcher and compressor systems (total ~0.4 m^2) are also quite modest. Also, using amplifier crystals with the maximum possible doping-level limits the material path length. In the final amplifier stage a relatively high pump fluence permits the use of a modest-size crystal (2-cm diameter, Union Carbide Corporation), which can be readily obtained with high optical quality. We found that the major limitation on focusability of the beam is the quality of the final amplifier crystal. However, it is likely that amplifiers with significantly higher pulse energies will require lower doping levels to avoid gain depletion that is due to transverse ASE. This requires a crystal with significantly larger total volume, making fabrication of high-optical-quality crystals progressively more challenging. The diffraction gratings used in this laser were found to have consistently high surface flatness, diffraction efficiency, and uniform reflectivity at modest cost.

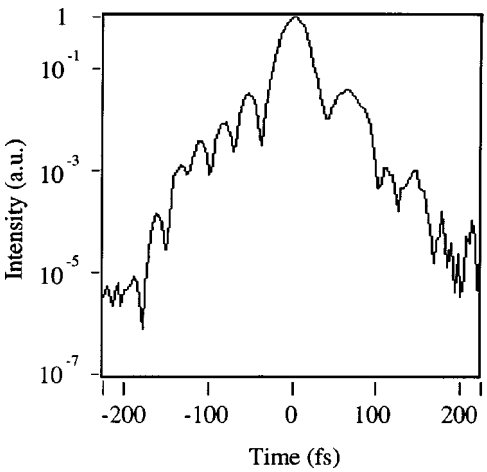

Fig. 4. High-dynamic-range pulse measurement with FROG.

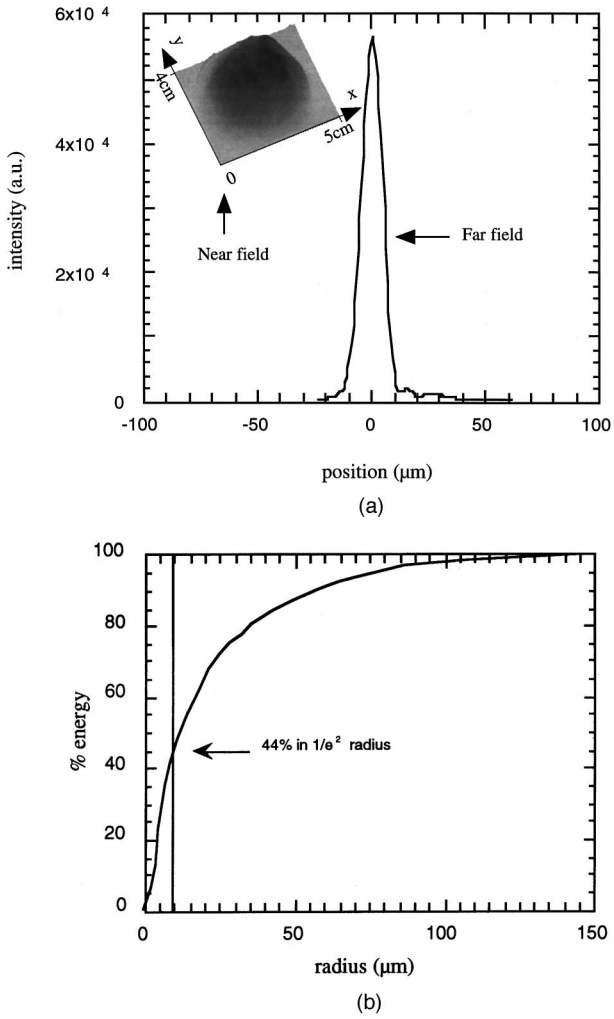

Fig. 5. (a) Near-field and far-field beam profiles; (b) percentage of energy as a function of radius from focus, as integrated from the CCD data. We took these data by focusing the beam onto a SpectraSource Instruments model MCD600S CCD with 16-bit dynamic range. The leveling off of this curve at a large radius, well before the edge of the CCD, indicates that the focal-spot image includes all the laser energy.

In conclusion, we have generated >40-TW peak-power pulses with an average power of 10 W, with 24-fs pulse duration, at a repetition rate of 10 Hz, and with very good beam quality. Optimal system designs allow us to maintain a low *B* integral and a compact size without compro-

mising the system performance. The power amplifier efficiency is close to 50%. The final output peak intensity is measured to be $1.4 \times 10^{19}\,\mathrm{W/cm^2}$ when focused by a 600-mm focal-length off-axis parabola, with a potential focusability well in excess of $10^{20}\,\mathrm{W/cm^2}$ when tighter focusing optics are used. This is a high peak-power laser system with simultaneously high focusability, high average power, and a short well-characterized pulsewidth.

REFERENCES

1. J. Zhou, C. P. Huang, M. M. Murnane, and H. C. Kapteyn, "Amplification of 26-fs, 2-TW pulses near the gain-narrowing limit in Ti:sapphire," Opt. Lett. **20**, 64–66 (1994).
2. J. P. Chambaret, C. Le Blanc, G. Cheriaux, P. Curley, G. Darpentigny, P. Rousseau, G. Hamoniaux, A. Antonetti, and F. Salin, "Generation of 25-TW, 32-fs pulses at 10 Hz," Opt. Lett. **21**, 1921–1923 (1996).
3. C. Barty, T. Guo, C. Le Blanc, F. Raksi, C. Rose-Petruck, J. Squirer, K. Wilson, V. Yakovlev, and K. Yamakawa, "Generation of 18-fs, multiterawatt pulses by regenerative pulse shaping and chirped-pulse amplification," Opt. Lett. **21**, 668–670 (1996).
4. J. Itatani, Y. Nabekawa, K. Kondo, and S. Watanabe, "Generation of 13-TW, 26-fs pulses in a Ti:sapphire laser," Opt. Commun. **134**, 134–138 (1997).
5. M. Yamakawa, S. Matsuoka, H. Takuma, C. Barty, and D. Fittinghoff, "Generation of 16-fs, 10-TW pulses at a 10-Hz repetition rate with efficient Ti:sapphire amplifiers," Opt. Lett. **23**, 525–527 (1998).
6. S. Backus, C. Durfee, M. Murnane, and H. Kapteyn, "High power ultrafast lasers," Rev. Sci. Instrum. **69**, 1207–1223 (1998).
7. K. Yamakawa, M. Aoyama, S. Matsuoka, T. Kase, Y. Akahane, and H. Takuma, "100-TW sub-20-fs Ti:sapphire laser system operating at a 10-Hz repetition rate," Opt. Lett. **23**, 1468–1470 (1998).
8. A. Rundquist, C. Durfee, Z. Chang, S. Backus, C. Herne, M. M. Murnane, and H. C. Kapteyn, "Phased-matched generation of coherent soft x-rays," Science **280**, 1412–1415 (1998).
9. I. P. Christov, M. M. Murnane, and H. C. Kapteyn, "High-harmonic generation of attosecond pulses in the 'single-cycle' regime," Phys. Rev. Lett. **78**, 1251–1254 (1997).
10. H. C. Kapteyn, L. D. Silva, and R. W. Falcone, "Short-wavelength lasers," Proc. IEEE **80**, 342–347 (1992).
11. B. Lemoff, G. Y. Gin, C. Gordon, C. Barty, and S. E. Harris, "Demonstration of a 10-Hz femtosecond pulse-driven xuv laser at 41.8 nm in Xe-IX," Phys. Rev. Lett. **74**, 1574–1577 (1995).
12. C. Siders, S. LeBlanc, D. Fisher, T. Tajima, M. Downer, A. Babine, A. Stepanov, and A. Sergeev, "Laser wakefield excitation and measurement by femtosecond longitudinal interferometry," Phys. Rev. Lett. **76**, 3570–3573 (1996).
13. D. Umstadter, S. Chen, A. Maksimchuk, G. Mourou, and R. Wagner, "Nonlinear optics in relativistic plasmas and laser wakefield acceleration of electrons," Science **273**, 472–475 (1996).
14. D. J. Kane and R. Trebino, "Characterization of arbitrary femtosecond pulses using frequency-resolved optical gating," IEEE J. Quantum Electron. **29**, 571–579 (1993).
15. C. G. Durfee III, S. Backus, M. M. Murnane, and H. C. Kapteyn, "Design and implementation of a TW-class high-average power laser system," IEEE J. Sel. Top. Quantum Electron. **4**, 395–406 (1998).
16. S. Backus, J. Peatross, C. Huang, H. Kapteyn, and M. Murnane, "Ti:sapphire amplifier producing millijoule-level, 21-fs pulses at 1 kHz," Opt. Lett. **20**, 2000–2002 (1995).
17. G. Taft, A. Rundquist, H. Kapteyn, I. Christov, M. Murnane, K. DeLong, D. Fittinghoff, M. Krumbugel, and R. Trebino, "Measurement of 10-fs laser pulses," J. Quantum Electron. **2**, 575–585 (1997).
18. C. Chang, H. Sardesai, and A. M. Weiner, "Dispersion-free fiber transmission for femtosecond pulses by use of a dispersion-compensating fiber and a programmable pulse shaper," Opt. Lett. **23**, 283–285 (1998).
19. E. Zeek, K. Maginnis, S. Backus, U. Russek, M. Murnane, G. Mourou, H. Kapteyn, and G. Vdovin, "Pulse compression by use of deformable mirrors," Opt. Lett. **24**, 493–495 (1999).